Supporting Information for

Reversible pH-modified Fluorescence Transition in the Block Copolymer Micelles Enwrapping with Zinc(II) Fluorescent Complex

Yumei Qin,[a] Shuangde Li,*[b] Jun Lu,*[a] Zhen Li,[a] and Xue Duan[a]

[a] *State Key Laboratory of Chemical Resource Engineering, Beijing University of Chemical Technology, Beijing 100029, P. R. China*

[b] *State Key Laboratory of Multi-phase Complex Systems, Institute of Process Engineering, Chinese Academy of Sciences, Beijing 100190, PR China.*

LIST OF CONTENTS

Figure S9. Polarized fluorescence profiles and anisotropic value for $Zn(BTZ)_2$ DMF solution.
Figure S10. (a) Reversibility transition from green to blue emission of $Zn(BTZ)_2$@PS-*b*-PAA micelles repeated for 20 times; (b) the PL intensity of $Zn(BTZ)_2$@PS-*b*-PAA micelles (stored at room temperature) recorded for 32 days.
Figure S11. PL emission spectra of $Zn(BTZ)_2$@PS-*b*-PAA micelles at pH = 6.0 and 9.0 under 340 and 390 nm excitation, respectively, THF as solvent for PS-*b*-PAA.
Figure S12. Power X-ray diffraction patterns of $Zn(BTZ)_2$ molecules and after grinding.
Figure S13. CPTOSS ^{13}C NMR spectra of $Zn(BTZ)_2$ molecules and after grinding.
Figure S14. SEM top view images of $(micelles/LDH)_n$ film with a) $n = 4$ and b) $n = 12$..
Figure S15. Absorption and PL emission spectra of $(micelles/PDDA)_n$ films.

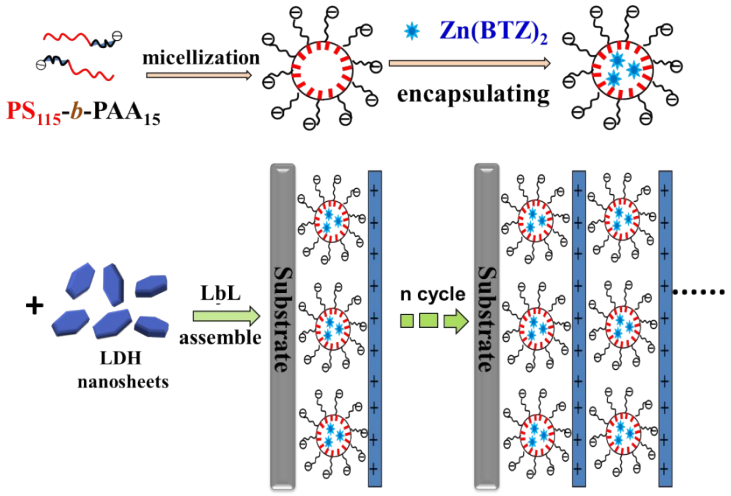

Scheme S1. Process scheme of formation of PS-*b*-PAA@$Zn(BTZ)_2$ micelle and fabrication of $(micelles/LDH)_n$ films.

1. Structure and Morphology Characterization for Micelles and $(micelles/LDH)_n$ Films

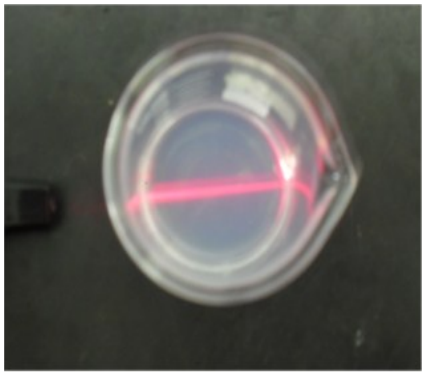

Figure S1. The photograph of $Zn(BTZ)_2$@PS-*b*-PAA micelles at pH = 6.0 with Tyndall effect.

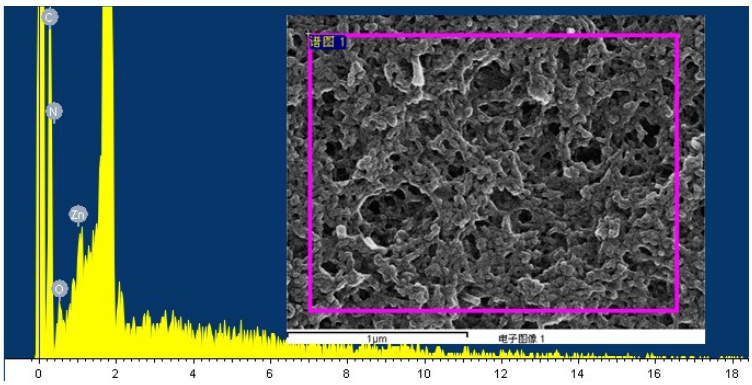

Figure S2. SEM-EDX analysis of $Zn(BTZ)_2$@PS-*b*-PAA micelles at pH = 7.5.

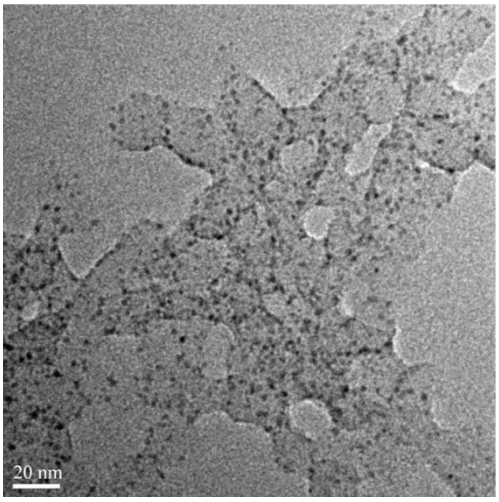

Figure S3. TEM image of $Zn(BTZ)_2$@PS-*b*-PAA micelles at pH = 7.5.

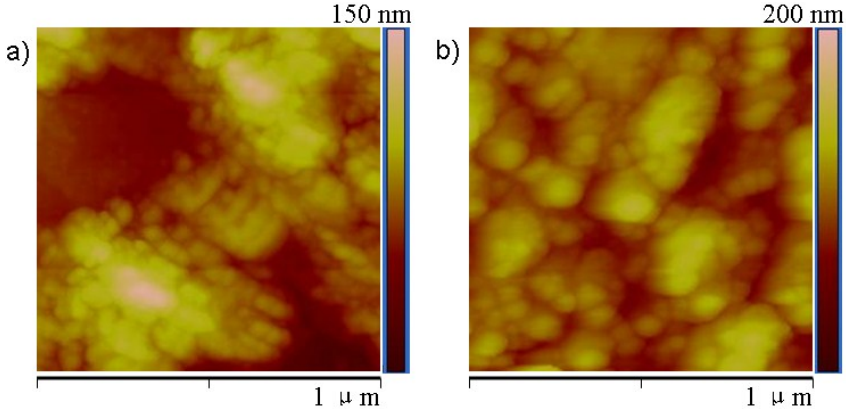

Figure S4. Tapping-mode AFM topographical 2D images of $Zn(BTZ)_2$@PS-*b*-PAA micelles: a) pH = 7.5 and b) pH = 9.0.

Atomic force microscope (AFM) images display that the individual micelle is spherical morphology and around 35 and 60 nm in diameter for pH = 7.5 and 9.0, respectively.

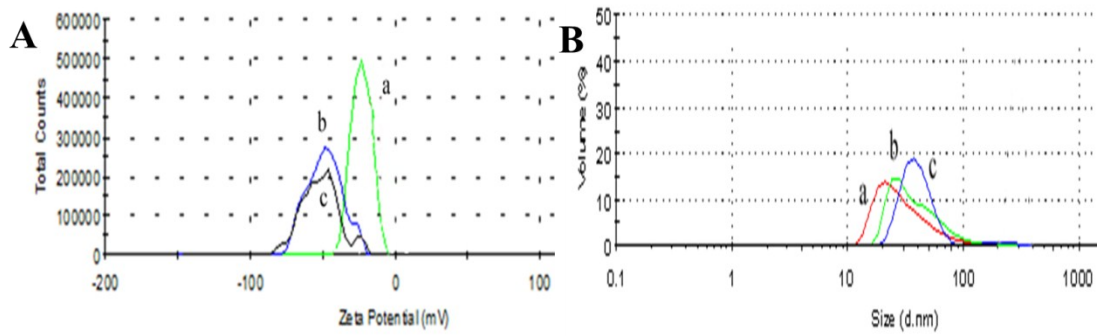

Figure S5. Zeta-potential and dynamic lighting scatting (DLS) diameter as a function of pH value of $Zn(BTZ)_2$@PS-*b*-PAA micelle: a, b, c) pH = 6.0, 7.5, 9.0, respectively.

2. pH-induced Photophysical Properties of $Zn(BTZ)_2$@PS-*b*-PAA Micelles and $(micelles/LDH)_n$ Films

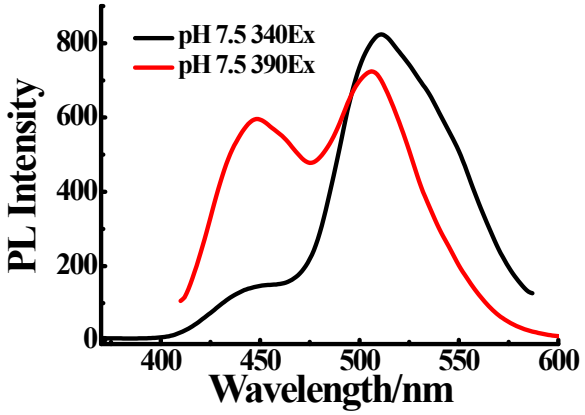

Figure S6. PL emission spectra of $Zn(BTZ)_2$@PS-*b*-PAA micelles at pH = 7.5 under 340 and 390 nm excitation.

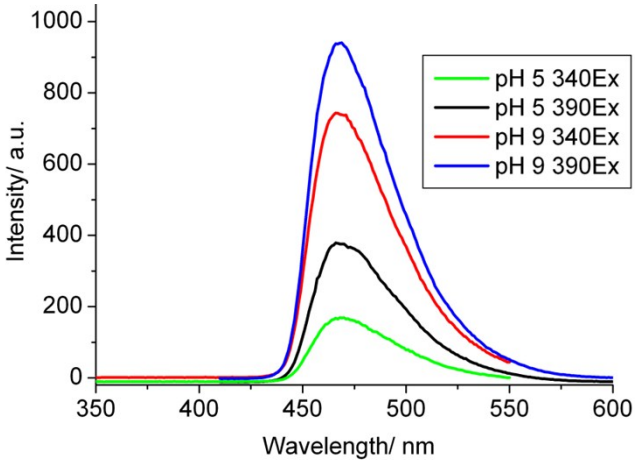

Figure S7. PL emission spectra of $Zn(BTZ)_2$ DMF solution at pH = 5.0 and 9.0 under 340 and 390 nm excitation, respectively.

Table S1. The single or double-exponential fitting of fluorescence decay data of $Zn(BTZ)_2$ solution, micelles and films under pH = 6.0, 9.0 at 375 nm laser excitation.

Samples	τ_i(ns)[a]	A_i(%)	$<\tau>$(ns)	χ^2[b]
$Zn(BTZ)_2$ DMF solution at 460 nm	4.53	100	4.53	1.29
$Zn(BTZ)_2$@PS-*b*-PAA micelles at 460 nm for pH = 9.0	4.06	100	4.06	1.21
$(Zn(BTZ)_2$@PS-*b*-PAA/LDH$)_{16}$ at 460 nm for pH = 9.0	2.06 5.16	57.94 42.06	3.36	1.09
$Zn(BTZ)_2$@PS-*b*-PAA micelles at 510 nm for pH = 6.0	0.69 4.29	15.59 84.41	3.73	1.20
$(Zn(BTZ)_2$@PS-*b*-PAA/LDH$)_{16}$ at 510 nm after HCl treatment	1.79 4.16	51.24 48.76	2.95	1.10

[a] τ_i(i = 1, 2) is the fitted fluorescence lifetime. A_i is the percentage of τ_i. In the biexponential case, $<\tau> = A_1\tau_1 + A_2\tau_2$; $A_1 + A_2 = 1$.).

[b] the goodness of fit is indicated by the value of χ^2.

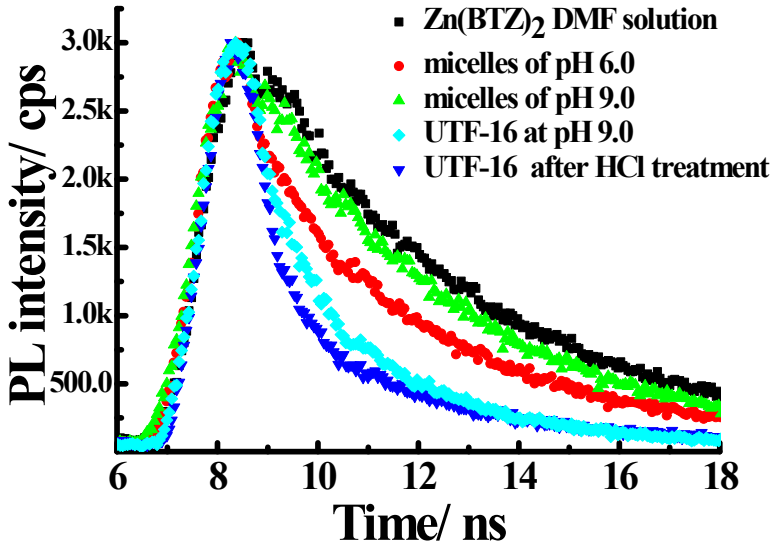

Figure S8. Fluorescence decay profile for $Zn(BTZ)_2$ DMF solution, $Zn(BTZ)_2$@PS-*b*-PAA micelles at pH 6.0 and 9.0, $(Zn(BTZ)_2$@PS-*b*-PAA/LDH$)_{16}$ film at pH 9.0 and the film exposed to HCl atmosphere for 2 mins.

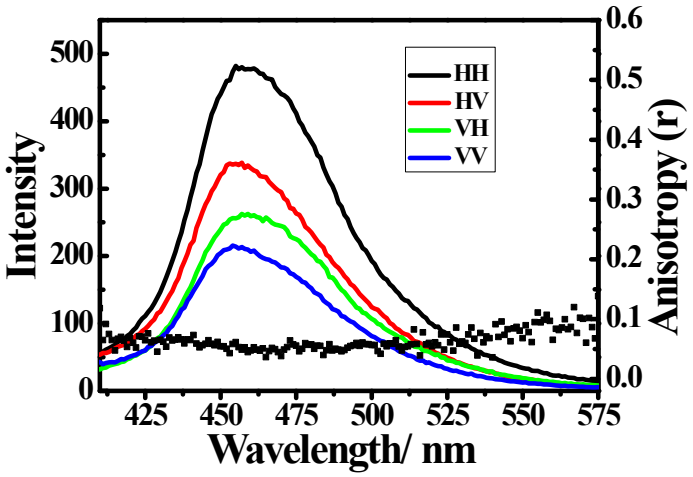

Figure S9. Polarized fluorescence profiles in the HH, HV, VV, VH modes and anisotropic value (*r*) for $Zn(BTZ)_2$ DMF solution under 390nm excitation.

The anisotropic value $r = (I_{VV}-GI_{VH})/(I_{VV} + 2GI_{VH})$, where $G = I_{HV}/I_{HH}$. I_{VH} donates the PL intensity obtained with vertical polarized excitation and horizontal polarized detection, and I_{VV}, I_{HH}, I_{HV} are defined similarly.

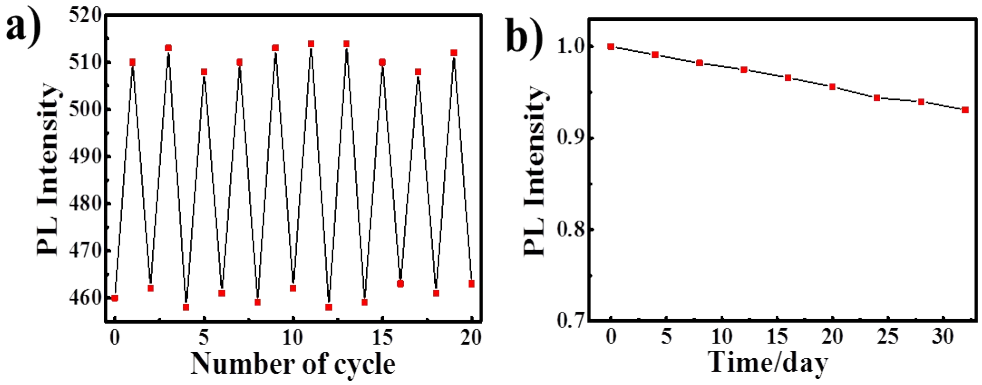

Figure S10. (a) Reversibility transition from green to blue emission of $Zn(BTZ)_2$@PS-*b*-PAA micelles repeated for 20 times; (b) the PL intensity of $Zn(BTZ)_2$@PS-*b*-PAA micelles (stored at room temperature) recorded for 32 days.

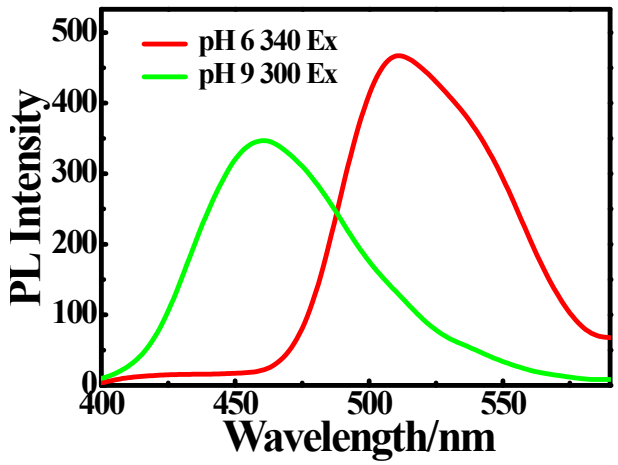

Figure S11. PL emission spectra of $Zn(BTZ)_2$@PS-*b*-PAA micelles at pH = 6.0 and 9.0 under 340 and 390 nm excitation, respectively, THF as solvent for PS-*b*-PAA.

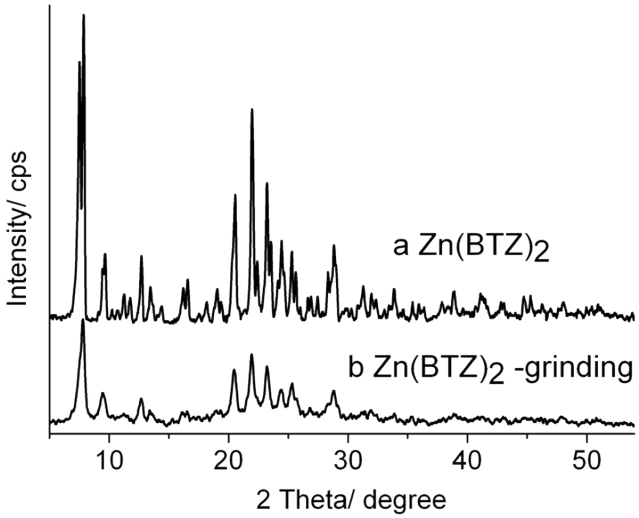

Figure S12. Power X-ray diffraction patterns of $Zn(BTZ)_2$ molecules and after grinding.

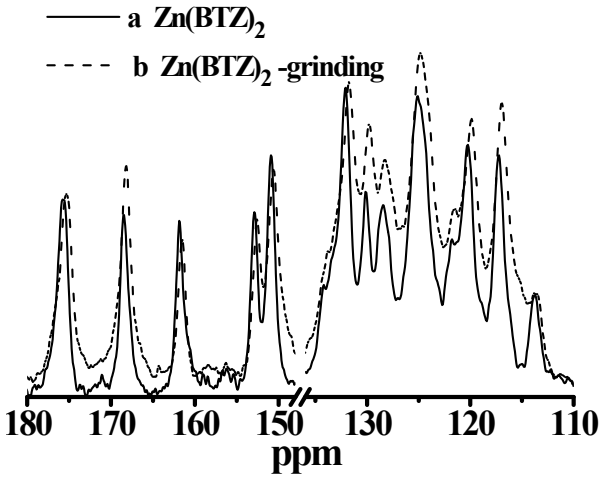

Figure S13. CPTOSS ^{13}C NMR spectra of $Zn(BTZ)_2$ molecules and after grinding.

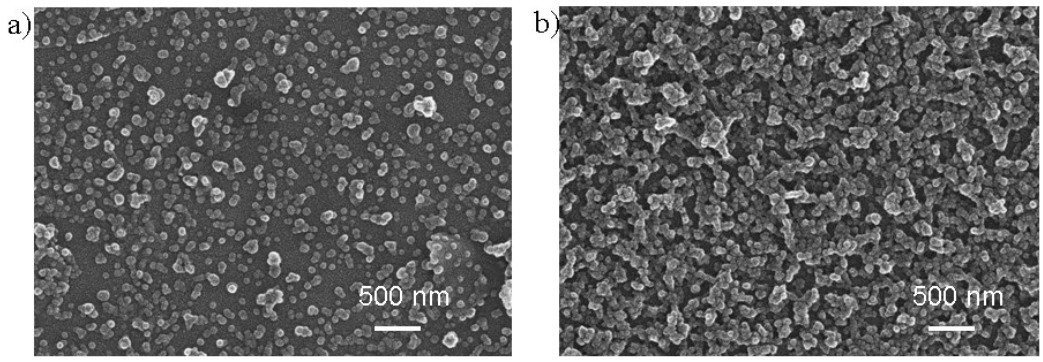

Figure S14. SEM top view images of $(micelles/LDH)_n$ film with a) $n = 4$ and b) $n = 12$.

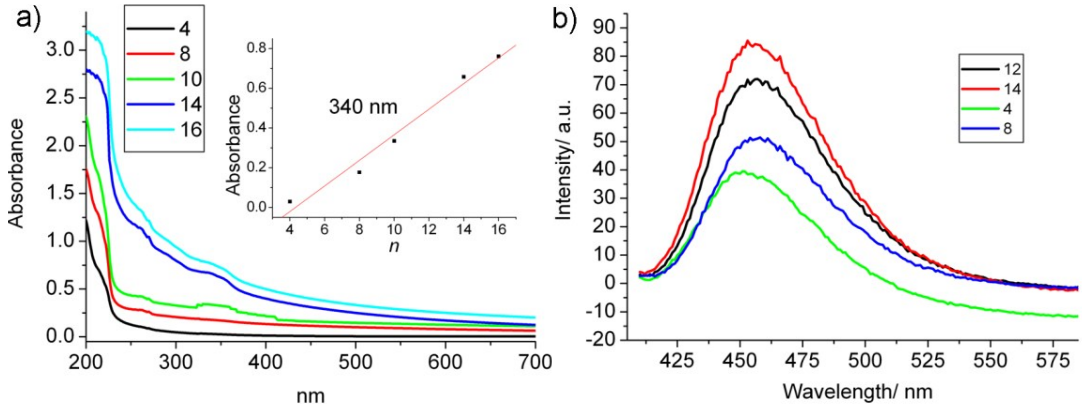

Figure S15. a) Absorption spectra of $(micelles/PDDA)_n$ films. The inset plots show the absorbance at 340 nm vs. the number of bilayers n. b) PL emission spectra of $(micelles/PDDA)_n$ films with variable bilayers under 390 nm excitation.